Downstream signaling of disease-associated mutations on GPR56/ADGRG1

Orkun Cevheroglu[1], Nil Demir[2], Seçkin Kesici[2], Salih Özçubukçu[2], and Çağdaş Son[2]

[1]Ankara University
[2]Middle East Technical University

January 10, 2023

Abstract

GPR56/ADGRG1 is an adhesion GPCR and mutations on this receptor cause cortical malformation due to the over-migration of neural progenitor cells on the brain surface. At the pial surface, GPR56 interacts with collagen III, induces Rho dependent activation through Gα12/13 and inhibits the neuronal migration. In human glioma cells, GPR56 inhibits cell migration through Gαq/11 dependent Rho pathway. GPR56-tetraspanin complex is known to couple with Gαq/11. GPR56 is an aGPCR that couples with various G proteins and signals through different downstream pathways. In this study, BFPP mutants disrupting GPR56 function but remain to be expressed on plasma membrane were used to study receptor signaling through Gα12, Gα13 and Gα11 with BRET biosensors. GPR56 showed coupling with all three G proteins and activated heterotrimeric G protein signaling upon stimulation with Stachel peptide. However, BFPP mutants showed different signaling defects for each G protein indicative of distinct activation and signaling properties of GPR56 for Gα12, Gα13 or Gα11. β-arrestin recruitment was also investigated following the activation of GPR56 with Stachel peptide using BRET biosensors. N-terminally truncated GPR56 showed enhanced β-arrestin recruitment, however neither wild-type receptor nor BFPP mutants gave any measurable recruitment upon Stachel stimulation, pointing different activation mechanisms for β-arrestin involvement.

ORIGINAL ARTICLE

Downstream signaling of disease associated mutations on GPR56/ADGRG1

Orkun Cevheroğlu[1, *] ? Nil Demir[2, *] ? Mehmet Seçkin Kesici[3] ? Salih Ozcubukcu[3] ? Cağdaş D. Son[2]

[1] Stem Cell Institute, Ankara University, Çankaya 06520 Ankara, Türkiye [2] Department of Biological Sciences, Middle East

INTRODUCTION

Bilateral frontoparietal polymicrogyria (*BFPP*) is an autosomal recessive genetic disorder, caused by the mutations in the GPR56/ADGRG1 gene located on human chromosome 16q21 [1, 2]. The genotype–phenotype analysis of *BFPP* patients yielded a cobblestone-like cortical malformation, which is characterized as formation of neuronal ectopias on the surface of the brain and aberrant migration of neural progenitor cells [3-5]. At the pial surface, the interaction of GPR56 with extracellular matrix protein collagen III activates the Rho signaling pathway through $G\alpha_{12/13}$ and this results in inhibition of the neuronal migration [6].

GPR56 is a member of the G protein-coupled receptor (GPCR) superfamily. In humans, over 800 members constitute this huge receptor superfamily, hallmarked by their 7-transmembrane (7TM) structure and ability

to couple heterotrimeric G proteins upon activation. GPCRs are involved in almost all biological processes with their pivotal role as cellular signal transduction of immensely diverse extracellular stimuli (i.e. photons, ions, small molecules, neurotransmitters, hormones and even mechanical stimuli) inside the cell. Mutations and functional problems in GPCRs are linked to many important human diseases [7]. Hence, taking part in almost all physiological processes and possessing druggable sites accessible at the cell surface have already made GPCRs targets of almost 40% of the prescribed drugs [8].

GPR56 is an adhesion GPCR (aGPCR) according to a further phylogenetic classification of GPCRs in the human genome [9, 10]. With 33 members, aGPCRs constitute the second largest GPCR family in humans. Almost all members in this receptor family have numerous splice variants and these receptor isoforms show tissue-dependent expression, various functions and different downstream signaling properties. All these features in aGPCRs adds another layer of complexity and structural variety to this enigmatic family of receptors [11-13]. Arguably, the most intriguing characteristics of aGPCRs are their extremely large N-terminus which consists of various protein domains that are involved in protein-protein, cell-cell and cell-matrix interactions and these multi-domain structures point to the multifaceted roles of this receptor family in signal transduction, modulation as well as cell adhesion [14, 15]. A very important characteristic feature of aGPCRs (except for GPR123/ADGRA1) is a highly conserved extracellular GPCR autoproteolysis-inducing (GAIN) domain [16]. In most aGPCRs, an autoproteolytic cleavage occurs at the GPCR proteolysis site (GPS) located within the GAIN domain, yielding non-covalently bound extracellular N-terminal fragment (NTF) and membrane integrated C-terminal fragment (CTF) composed of 7TM structure and the*Stachel* peptide [17-22].

Activation of GPCRs on the extracellular side causes conformational changes that facilitate the interaction of receptors with G proteins or β-arrestins at the cytosolic side of the plasma membrane and mediate the downstream signaling pathways. Elucidating the molecular mechanisms of receptor activation and signaling with high spatiotemporal resolution is very crucial for GPCRs due to their pivotal roles in many physiological processes, their related pathologies, therapeutic relevance and druggability. During the past recent years, there has been a considerable effort to develop bioluminescent or fluorescent biosensors working on the principles of resonance energy transfer (RET) for the real-time monitoring of the GPCR activation in live cells [23-25]. These systems were successfully applied to study the activation of numerous GPCRs, their coupling with G proteins and recruitment of β-arrestins [26, 27].

In this work, the effects of *BFPP* mutations on GPR56 signaling upon *Stachel* peptide activation with $G\alpha_{12}$, $G\alpha_{13}$ and $G\alpha_{11}$ were studied using BRET biosensors. In principle, biosensors used are based on the $G\beta\gamma$ dissociation from the G protein α-subunit upon GPCR activation in the exogenous expression of G protein-coupled receptor kinase (GRK) [28, 29]. β-arrestin recruitment BRET biosensor was employed to investigate the effects of disease-associated mutations on the arrestin recruitment for *Stachel* peptide activated receptors [30].

MATERIAL AND METHODS

The study was conducted in accordance with the Basic & Clinical Pharmacology & Toxicology policy for experimental and clinical studies [31].

Chemical reagents and other materials

General laboratory chemicals were purchased from Sigma–Aldrich (Darmstadt, Germany) or Merck (Darmstadt, Germany). Cell culture media components, Lipofectamine LTX Reagent with PLUS, GeneJET Plasmid Miniprep Kit, GeneJET PCR Purification Kit were purchased from Thermo Fisher Scientific (MA, USA) or Invitrogen (MA, USA). Q5 Hot Start High-Fidelity DNA Polymerase was purchased from New England Biolabs (MA, USA). Primers used in this study were purchased from IDT Europe (Munich, Germany).

Protease inhibitor cocktail tablets were from Roche Diagnostics, (Mannheim, Germany). Antibodies (anti-GPR56, anti-β-actin and secondary horseradish peroxidase conjugated antibody) were from Santa Cruz Biotechnology (TX, USA). Immobilon-P membrane was from Millipore (Millipore Corporation, Bedford, MA). ECL reagent was from Pierce (MA, USA). White 96-well Lumitrac microplates were purchased from Greiner Bio-One (Kremsmünster, Austria), Nano-Glo®Luciferase Assay System which includes Furimazine was from Promega (Promega, USA), Coelenterazine was from Invitrogen (MA, USA). Berthold Mithras^2 LB 943 multimode plate reader was used in bioluminescence/fluorescence based experiments.

Synthesis of P7 *Stachel*peptide

The *Stachel* peptide for GPR56 P7, "*TYFAVLM* " was synthesized using solid phase peptide synthesis based on Fmoc strategy using HBTU and DIEA as the coupling agents. 20% piperidine-DMF solution was used as deprotection solution for Fmoc group and Rink amide resin was used as solid support. To cleave the side chain protecting groups and the peptide from resin, TFA-TIPS-H_2O (95 : 2.5 : 2.5) system was used. Analytical HPLC was performed on a Dionex instrument, with ThermoScientific ODS Hypersil, 5µ C18 column. 0.1% TFA-water as solvent A and 0.08% TFA-acetonitrile as solvent B were used. The gradient was 0-90% B 20 min and peptide was used without the necessity of any further purification. The purity of synthesized peptide was >90%.

DNA Constructs

The plasmid carrying the full-length human cDNA of GPR56/ADGRG1 was a generous gift from Assoc. Prof. Dr. Demet Araç (University of Chicago, USA). GRK-based G protein BRET biosensors (Venus 156-239-Gβ1, Venus 1-155-Gg2 and masGRK3ct-NanoLuc) were kind gifts from Prof. Dr. Kirill Martemyanov (University of Florida, USA). Finally, β-arrestin BRET biosensors (Rluc8-Arrestin-3-Sp1 and mem-linker-citrine-SH3) were generously donated by Prof. Dr. Nevin A. Lambert (Augusta University, USA).

Site directed mutagenesis

Five missense mutations from *BFPP* patients, which were shown not to fully block the surface expression of GPR56 [32] were introduced using site-directed mutagenesis with the double primer method. For this, both forward and reverse primers were designed to carry the targeted base change and to prevent the primer-primer dimers, eight non-overlapping bases were introduced at the 3' end of each primer. All primers used in the mutagenesis are shown in Table 1 (see supplementary materials for more). All constructs were verified by sequencing.

Table List of primers used to construct BFPP mutants of GPR56. For each mutation first lane corresponds forward primer, second lane gives reverse primer. All primers were given in 5' > 3'.

Change in amino acid	**Change in base**	**Primer Sequence (5' > 3')**
R38W	112C>T	tgcagccag**t**ggaaccagacacacaggagc
		ctggttcc**a**ctggctgcagaagcgaaagtc
Y88C	263A>G	aggggcctct**g**ccacttctgcctctactggaac
		gcagaagtgg**c**agaggcccctggggtcagg
C91S	272G>C	ctctaccacttct**c**cctctactggaaccgacatgctggg
		ccagtagagg**g**agaagtggtagaggcccctggg
R565W	1693C>T	gtgctggatc**t**gggactccctggtcagctac
		cagggagtccc**a**gatccagcacatggaagg
L640R	1919T>G	cttgtcgtcc**g**ctacctttcagcatcatcacc
		gaaaaggtag**c**ggacgacaagctggaaggtgcc

Cell culture and transient transfection of HEK293 cells

Human embryonic kidney cells (HEK293) were maintained in a humidified incubator with 5% CO_2 and 90% humidity at 37 °C. Cells were grown as a monolayer in Dulbecco's modified Eagle's medium (DMEM) with high glucose (25 mM) and pyruvate (1mM) supplemented with 10% (v/v) fetal bovine serum, 100 units/mL penicillin and 0.1 mg/mL streptomycin. Cells were regularly tested for mycoplasma contamination (EZ-PCR Mycoplasma Detection Kit, Kibbutz Beit-Haemek, Israel). For experiments, cells were seeded at a density of 2x$10^5$to each well of the clear 24-well plate. Before transient transfection cells were grown to 60 to 80% confluence. Transfection was performed using Lipofectamine LTX with PLUS transfection reagent according to the manufacturer's instructions. Biosensors were used in transfection as explained in the previous reports [28-30]. Assays were performed 24h after transfection as confluency reaches 80%.

Membrane preparation and Western blot analysis

Cells were washed with ice-cold PBS buffer and lysed with RIPA buffer (50 mM Tris-HCl pH 8.0, 150 mM NaCl, 1% Nonidet P-40 (NP-40), 0.1% SDS, 0.5% sodium deoxycholate, 1mM EDTA, 1 mM DTT, 0.5 mM PMSF, 50 mM Na β-glycerophosphate, 1 mM NaF and 1× Protease inhibitor cocktail tablet). Extracts were centrifuged for 30 minutes at 16,000×g at 4°C. Protein concentration was measured with Pierce BCA (Bicinchoninic acid) protein assay kit. Membrane proteins were solubilized in SDS sample buffer and 20 µg of total protein from cells expressing GPR56 constructs were resolved by SDS-PAGE and transferred to Immobilon-P PVDF membrane (Millipore Corporation, USA) Blotting membranes were blocked with 5% non-fat dry milk in TBST for 1 hour at room temperature and followed by 3 washes with TBST. Blotting membranes were incubated with 1:500 diluted anti-GPR56 or anti-β-actin primary antibodies overnight at 4°C. Next day, blotting membranes were washed 3 times with TBST and incubated with 1:7500 diluted HRP conjugated secondary antibody for 1 hour at room temperature. After the secondary antibody incubation, blotting membranes were washed with TBST and briefly incubated with SuperSignal West Pico PLUS Chemiluminescent Substrate (Pierce, USA) according to the manufacturer's instructions. Blots were imaged using ChemiDocTM MP imaging system (BioRad, USA).

$G\alpha_{12}$, $G\alpha_{13}$, $G\alpha_{11}$ BPET biosensor assay

For Gα BRET biosensor assay, HEK293 cells were washed with BRET buffer [29] and gently detached from 24-well plate on the day of the assay. Cells were centrifuged at 900 rpm for 5 minutes and 7.5×10^4 HEK293 cells were seeded into each well of a white opaque 96-well microplate. Triplicate wells were loaded with P7*Stachel* peptide (*TYFAVLM*) with a final concentration of 1mM and 1:1000 ratio of Furimazine. After 5 minutes of incubation in the dark, bioluminescence and fluorescence signals were measured using Berthold Mithras^2 LB 943 multimode plate reader using MicroWin 2010 software (Berthold Technologies, Germany) equipped with high-efficiency BRET filters. For Nluc emission, NanoBRET filter (460nm/70) and for Venus emission, eYFP (540nm/40) filters were used in biosensor-based BRET experiments. Data acquired represents at least from three independent experiments done in triplicates. The statistical evaluation of quiescent receptor vs. *Stachel* stimulation within each construct was done by multiple t test. The comparison of each*BFPP* mutant with the *wild-type* GPR56 was done using ordinary one-way ANOVA and Dunnett's multiple comparison tests.

β-Arrestin BPET biosensor assay

For β-arrestin recruitment BRET biosensor assay, HEK293 cells were washed with BRET buffer and gently detached from 24-well plate on the day of the assay. Cells were centrifuged at 900rpm for 5 minutes and 7.5×10^4 HEK293 cells were seeded into each well of a white opaque 96-well microplate. Wells were loaded with P7*Stachel* peptide (*TYFAVLM*) to give a final concentration of 1 mM and with Coelenterazine native to yield a final concentration of 5 µM per well. After 5 minutes of incubation in the dark, bioluminescence and fluorescence signals were measured using Berthold Mithras^2 LB 943 multimode plate reader using MicroWin

2010 software (Berthold Technologies, Germany) equipped with high-efficiency BRET filters. For Citrine emission, eYFP filter (540nm/40) and for RLuc8 emission, Coelenterazine filter (480nm/20) were used in experiments. Data acquired represents at least from three independent experiments done in triplicates. The statistical evaluation of quiescent receptor vs. *Stachel* stimulation within each construct was done by multiple t test. The comparison of each*BFPP* mutant with the *wild-type* GPR56 was done using ordinary one-way ANOVA and Dunnett's multiple comparison tests.

RESULTS

Expression of BFPP mutant receptors

GPR56 or GPR56R38W, GPR56Y88C, GPR56C91S, GPR56R565W, GPR56L640R*BFPP* mutants were expressed in HEK293 cells by transient transfection (Figure 1). It was previously reported that GPR56 is fully cleaved from the GPS in HEK293 cells [33]. Under the SDS PAGE conditions reported herein, the non-covalent interactions between NTF and CTF were lost and only the receptor NTF was detected with the expected size around 55kDa using anti-GPR56 antibody which recognizes the NTF of the receptor. A decrease in the expression for all*BFPP* mutant receptors was observed compared with the*wild-type* GPR56. All *BFPP* mutants used in this study were previously reported to be expressed on the cell surface [32].

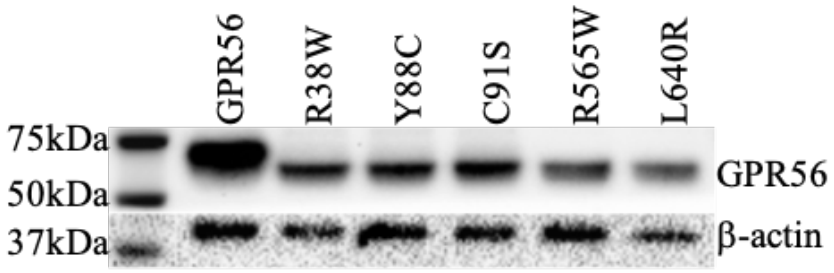

Figure Western blot showing the expression of GPR56 and the BFPP mutants in transiently transfected HEK293 cells. The first row corresponds to the expression of GPR56 and the mutant receptors detected by anti-GPR56 antibody targeting the NTF. The lower row corresponds to β-actin expression detected by anti-β-actin antibody.

Τηε εφφεςτ οφ ΒΦΠΠ μυτατιονς ον Γα$_{12}$ςουπλινγ

GPR56 or GPR56R38W, GPR56Y88C, GPR56C91S, GPR56R565W, GPR56L640R*BFPP* mutants were co-expressed with Gα_{12} and GRK-based G$\beta\delta$ biosensors to assess the effect of each mutation on the G protein coupling, upon receptor activation with the *Stachel*peptide. For this, HEK293 cells were treated with 1mM P7 *Stachel*peptide and Gα_{12} coupling and heterotrimeric G protein activation was measured as nanoBRET signal. The most severe coupling defect between the receptor and Gα_{12} was observed for GPR56L640R ($p<0.01$ compared with GPR56). Gα_{12}coupling defects were also measured for GPR56R565W ($p<0.01$ compared with GPR56) and GPR56C91S ($p<0.01$ compared with GPR56). GPR56R38W and GPR56Y88C *BFPP* mutants showed Gα_{12} coupling upon *Stachel* peptide stimulation with no significant change compared with the *wild-type* receptor.

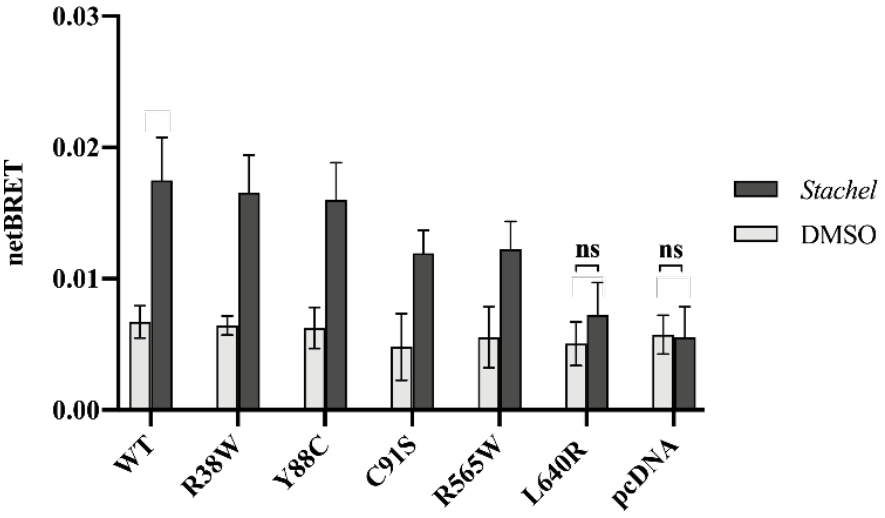

Figure The coupling of Stachel-activated GPR56 and disease associated mutations of the receptor with $G\alpha_{12}$.

Тне ефφецт оφ ВΦПП μутатионς он Гα$_{13}$ςоупλинγ

GPR56 or *BFPP* mutants of the receptor were co-expressed with $G\alpha_{13}$ and GRK-based $G\beta\delta$ biosensors to assess the effect of each mutation on the $G\alpha_{13}$ protein coupling, upon receptor activation with the *Stachel* peptide. For this, HEK293 cells were treated with the 1mM P7 *Stachel* peptide and $G\alpha_{13}$ coupling and heterotrimeric G protein activation was measured as nanoBRET. Under the biosensor conditions reported in this work, all *BFPP* mutants showed disrupted $G\alpha_{13}$coupling while the most severe was observed for GPR56R38W.

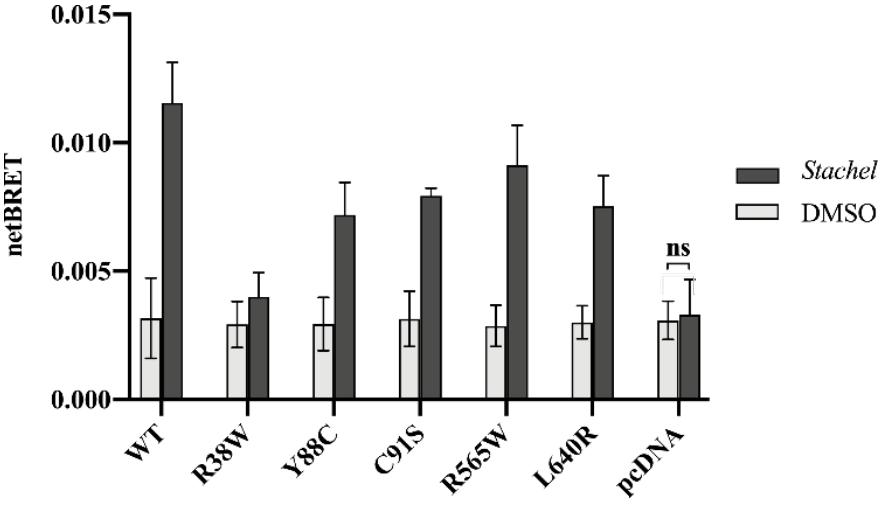

Figure The coupling of Stachel-activated GPR56 and disease associated mutations of the receptor with $G\alpha_{13}$.

Тне ефφецт оφ ВΦПП μутатионς он Гα$_{11}$ςоупλинγ

GPR56 was previously shown to couple with $G\alpha_{q/11}$ as a GPR56-CD81-$G\alpha_{q/11}$ complex [34]. In human glioma cells, stimulation of GPR56 with its agonistic monoclonal antibodies resulted in signaling through $G\alpha_q$ dependent Rho pathway [35]. GPR56 or *BFPP* mutants of the receptor were co-expressed with $G\alpha_{11}$ and

GRK-based Gβδ biosensors to assess the effect of each mutation on the G protein coupling when the receptor is stimulated with its *Stachel* peptide. For this, HEK293 cells were treated with the 1mM P7 *Stachel* peptide and $G\alpha_{11}$coupling and heterotrimeric G protein activation was measured as nanoBRET signal. GPR56C91S gave statistically indistinguishable nanoBRET compared with *wild-type* receptor. A decrease in nanoBRET indicative of G protein coupling defect was measured in all other*BFPP* mutants, however GPR56R565W did not show any $G\alpha_{11}$ coupling.

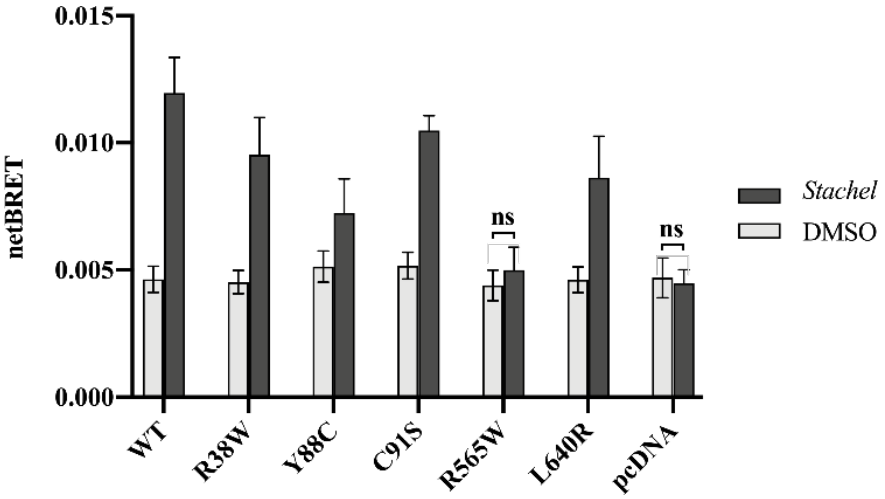

Figure The coupling of Stachel activated GPR56 and BFPP associated mutations of the receptor with $G\alpha_{11}$.

Τηε εφφεςτ οφ ΒΦΠΠ μυτατιονς ον β-Αρρεστιν ρεςρυιτμεντ

It was previously reported that NTF truncated human GPR56 from amino acids 1–342 gave enhanced interactions with β-arrestin compared to the full-length receptor [36]. In this work, GPR56 or *BFPP*mutants of the receptor were co-expressed with β-arrestin (Rluc8-arrestin3-Sp1) and GRK-based biosensors [30] to assess the effect of each mutation on the β-arrestin recruitment, upon receptor activation with the *Stachel* peptide. For this, HEK293 cells were treated with 1mM P7 *Stachel* peptide and β-arrestin recruitment was measured as a BRET signal. The arrestin biosensor assay utilized in this study gave increased plasma membrane recruitment for the NTF truncated GPR56 however stimulation of *wild-type* receptor or*BFPP* mutants with the *Stachel* peptide did not lead to any measurable recruitment.

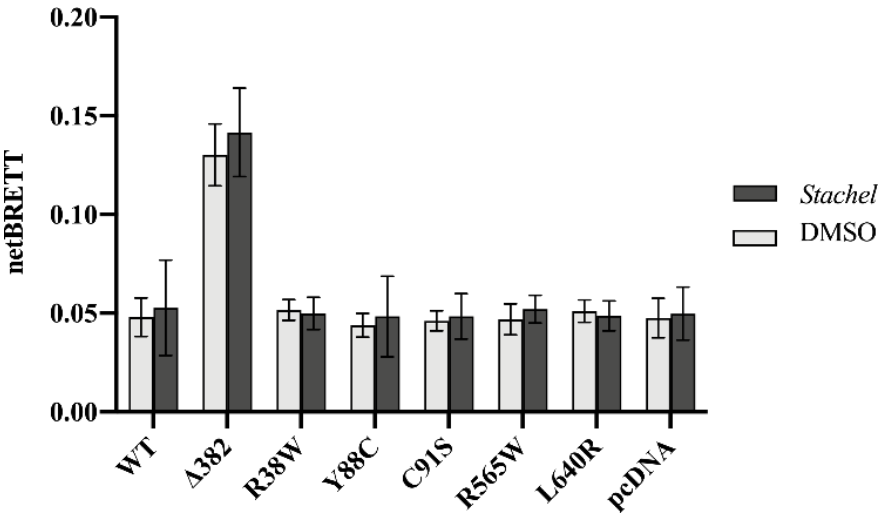

Figure β-arrestin recruitment of the Stachel-activated GPR56 and BFPP associated mutants of the receptor.

DISCUSSION

GPR56 is known to be involved in a wide range of physiological processes in the nervous system, immune system, male reproductive organs, hematopoietic stem and progenitor cells; functional problems with the receptor result in pathologies such as *Bilateral frontoparietal polymicrogyria (BFPP)* , depression and arguably GPR56 is the most studied aGPCR in cancer [37]. *BFPP* is a monogenetic disease resulting in a severe brain malformation and several mutations in GPR56 were found in patients diagnosed with *BFPP* [2]. In this work, five missense *BFPP* mutations on GPR56 were chosen that were previously reported to be expressed on the plasma membrane [32]. From those, R38W, Y88C and C91S are found on the NTF of the receptor; R565W is located on the 2nd extracellular loop and L640R is on the 3rd extracellular loop.

GPR56 is known to inhibit neural progenitor cell migration by coupling with $G\alpha_{12/13}$ and inducing Rho dependent activation of the transcription mediated through the serum-response element (SRE) and NF-κB-responsive element resulting in an actin fiber reorganization [38]. GPR56 is also known to form a complex with tetraspanin proteins CD9 and CD81 on the plasma membrane and this complex couples with $G\alpha_{q/11}$ and Gβ subunits [34]. Agonistic monoclonal antibodies generated towards the NTF of GPR56 resulted in the inhibition of human glioma cell migration through the $G\alpha_q$ dependent Rho pathway [35]. GPR56 was also reported to promote myoblast fusion through SRE and nuclear factor of activated T-cell (NFAT) mediated signaling [39]. Expression of GPR56 into HEK293 cells is known to lead $G\alpha_{12/13}$ activation and induce Rho dependent stimulation of SRE [38], however the Rho, SRE or NFAT mediated downstream signaling studies fail to discriminate between $G\alpha_{12}$ and $G\alpha_{13}$ signaling, which were known to have distinct physiological roles [40-42]. Furthermore, Gβγ and $G\alpha_{q/11}$ was also reported to induce Rho activation [43, 44].

GPR56 has numerous interacting partners such as collagen III [6], tissue transglutaminase (TG2) [45], and laminin [46]; the receptor was also previously reported to be activated by its*Stachel* peptide (*TYFAVLM*) [20]. In the current work, the coupling of GPR56 with $G\alpha_{12}$, $G\alpha_{13}$and $G\alpha_{11}$ upon the receptor activation with its*Stachel* peptide and the effects of *BFPP* mutants on G protein coupling was studied. For this, nanoBRET based biosensor system was chosen that is suitable for untagged receptor, untagged Gα, Venus tagged Gβ1γ2 and masGRK3ct-Nluc which is composed of G protein-coupled receptor kinase 3 carrying a myristic acid plasma membrane attachment peptide tagged with Nluc [28].

Under the biosensor conditions reported in this study, stimulation of GPR56 with its *Stachel* peptide showed G protein coupling and heterotrimeric G protein activation for $G\alpha_{12}$, $G\alpha_{13}$ and $G\alpha_{11}$. However, GPR56*BFPP*

mutants showed different coupling defects for each G protein α-subunit. Coupling between GPR56 and $G\alpha_{12}$ was disrupted in both extracellular loop *BFPP* mutations (GPR56L640R and GPR56R565W); on the other hand, receptor $G\alpha_{13}$ coupling and heterotrimeric G protein activation was measured for the extracellular loop receptor mutants. These results indicate the distinct signaling roles of GPR56 with $G\alpha_{12}$ or $G\alpha_{13}$. *Stachel* peptide stimulation of the receptor also showed measurable $G\alpha_{11}$ activation in the biosensor assay reported herein. GPR56 activation was shown to lead $G\beta\gamma$ subunit dissociation from $G\alpha_{11}$ and liberated $G\beta\gamma$ activates the calcium channels [33]. The working principle of the biosensor in this study relies on the change in nanoBRET upon dissociation of $G\beta\gamma$ from $G\alpha$ as a result of receptor activation. While the results confirmed the previous findings, studying *BFPP* mutants provided further insights into $G\alpha_{11}$ signaling. The most severe disruption was observed between GPR56R565W and $G\alpha_{11}$ coupling. All*BFPP* mutants showed disrupted coupling with $G\alpha_{11}$and heterotrimeric G protein activation except for GPR56C91S. In sum, stimulation of GPR56 with its *Stachel* peptide resulted in measurable activation in $G\alpha_{12}$, $G\alpha_{13}$ and $G\alpha_{11}$ signaling however, *BFPP* mutations resulted in distinctly different effects for each signaling pathway. It is noteworthy to mention at this point that, the data supplied in this study reflects the activation of GPR56 with its *Stachel* peptide, collagen III or TG2 treatment will provide more insights about the signaling of this receptor.

In the second part of the study, β-arrestin recruitment of GPR56 or*BFPP* mutants was measured upon activation of the receptor with its *Stachel* peptide. For this, a BRET based biosensor suitable for untagged receptors that measures the translocation of β-arrestin to the plasma membrane upon receptor activation was utilized. In the biosensor design, Rluc8 tagged β-arrestin and membrane-bound citrine fluorescent protein were used and the recruitment of β-arrestin was measured as a BRET increase in the exogenous expression of G protein-coupled receptor kinase 2 [30]. It was previously reported that NTF truncated GPR56 showed enhanced binding with β-arrestin [33, 36]. In accordance with the previous findings, NTF truncated GPR56 gave enhanced β-arrestin recruitment to the plasma membrane, however*Stachel* peptide stimulation of neither GPR56 nor *BFPP*mutants showed any significant change in β-arrestin recruitment. These results point to a different receptor activation mechanism for β-arrestin possibly through the activation of GPR56 with other ligands/interacting partners.

The complex architecture of aGPCRs arises from their extremely large NTFs. These structures carry various protein domains that are involved in diverse array of protein interactions including the extracellular matrix proteins; cell-cell interactions and cell adhesion. Some members of this enigmatic family of receptors were also shown to be involved in sensing the mechanical stimuli at the cellular level [18, 47-49]. Adhesion GPCRs also function like classical GPCRs, signaling canonically through their CTF domains that couple with and activate heterotrimeric G proteins. Hence, our current knowledge points to the multifaceted and multi-functional roles of this receptor family in signal transduction and modulation [14, 15]. The results reported in this study measured the direct coupling of three G proteins, $G\alpha_{12}$, $G\alpha_{13}$ and $G\alpha_{11}$ with GPR56 and the heterotrimeric G protein activation. Previous reports on GPR56 signaling rely mostly on the Rho dependent activation of further downstream elements rather than the direct G protein activation. Studying the downstream signaling defects of the disease associated mutations of GPR56 indicated that the receptor has distinct activation and signaling properties for each G protein and mutations located in various compartments of the receptor showed distinctly different coupling disruptions. In β-arrestin recruitment assays, NTF truncated receptor showed enhanced β-arrestin translocation to the plasma membrane, however stimulation of *wild-type* GPR56 or *BFPP* mutants with the*Stachel* peptide did not result in any recruitment. These results might indicate that β-arrestin recruitment possibly require different activation mechanisms.

The BRET based biosensors used in this study showed the direct coupling of GPR56 with $G\alpha_{12}$, $G\alpha_{13}$ and $G\alpha_{11}$ and the heterotrimeric G protein activation. Also, BRET based β-arrestin biosensor measured an enhanced recruitment of the NTF truncated receptor as previously reported. Considering the rich physiology and related pathologies of GPR56, the biosensors utilized in this work can further be applied for studying the mechanisms of receptor activation through different interacting partners and applied for drug screening studies.

ACKNOWLEDGEMENTS

We kindly thank Dr. Demet Araç for gifting us the human GPR56 cDNA. We also thank Dr. Kirill Martemyanov and Dr. Nevin A. Lambert for sending us the biosensors. This study received financial support from The Scientific and Technological Council of Turkey.

CONFLICT OF INTEREST

The authors declare no conflict of interest.

ORCID

Orkun Cevheroğlu https://orcid.org/0000-0002-3895-8869

Salih Özçubukçu https://orcid.org/0000-0001-5981-1391

Çağdaş D. Son https://orcid.org/0000-0002-4076-5441

REFERENCES

1. Piao X, Basel-Vanagaite L, Straussberg R, Grant PE, Pugh EW, Doheny K, et al. An autosomal recessive form of bilateral frontoparietal polymicrogyria maps to chromosome 16q12.2-21. Am J Hum Genet. 2002;70:1028-33.

2. Piao X, Hill RS, Bodell A, Chang BS, Basel-Vanagaite L, Straussberg R, et al. G protein-coupled receptor-dependent development of human frontal cortex. Science. 2004;303:2033-6.

3. Piao X, Chang BS, Bodell A, Woods K, Benzeev B, Topcu M, et al. Genotype-phenotype analysis of human frontoparietal polymicrogyria syndromes. Ann Neurol. 2005;58:680-7.

4. Li S, Jin Z, Koirala S, Bu L, Xu L, Hynes RO, et al. GPR56 regulates pial basement membrane integrity and cortical lamination. J Neurosci. 2008;28:5817-26.

5. Bahi-Buisson N, Poirier K, Boddaert N, Fallet-Bianco C, Specchio N, Bertini E, et al. GPR56-related bilateral frontoparietal polymicrogyria: further evidence for an overlap with the cobblestone complex. Brain. 2010;133:3194-209.

6. Luo R, Jeong SJ, Jin Z, Strokes N, Li S, Piao X. G protein-coupled receptor 56 and collagen III, a receptor-ligand pair, regulates cortical development and lamination. Proc Natl Acad Sci U S A. 2011;108:12925-30.

7. Hauser AS, Chavali S, Masuho I, Jahn LJ, Martemyanov KA, Gloriam DE, et al. Pharmacogenomics of GPCR Drug Targets. Cell. 2018;172:41-54.e19.

8. Hauser AS, Attwood MM, Rask-Andersen M, Schioth HB, Gloriam DE. Trends in GPCR drug discovery: new agents, targets and indications. Nat Rev Drug Discov. 2017;16:829-42.

9. Fredriksson R, Lagerstrom MC, Lundin LG, Schioth HB. The G-protein-coupled receptors in the human genome form five main families. Phylogenetic analysis, paralogon groups, and fingerprints. Mol Pharmacol. 2003;63:1256-72.

10. Schioth HB, Fredriksson R. The GRAFS classification system of G-protein coupled receptors in comparative perspective. Gen Comp Endocrinol. 2005;142:94-101.

11. Bjarnadottir TK, Geirardsdottir K, Ingemansson M, Mirza MA, Fredriksson R, Schioth HB. Identification of novel splice variants of Adhesion G protein-coupled receptors. Gene. 2007;387:38-48.

12. Knierim AB, Röthe J, Çakir MV, Lede V, Wilde C, Liebscher I, et al. Genetic basis of functional variability in adhesion G protein-coupled receptors. Sci Rep. 2019;9:11036.

13. Rosa M, Noel T, Harris M, Ladds G. Emerging roles of adhesion G protein-coupled receptors. Biochem Soc Trans. 2021;49:1695-709.

14. Liebscher I, Cevheroglu O, Hsiao CC, Maia AF, Schihada H, Scholz N, et al. A guide to adhesion GPCR research. FEBS J. 2021.

15. Yona S, Lin HH, Siu WO, Gordon S, Stacey M. Adhesion-GPCRs: emerging roles for novel receptors. Trends Biochem Sci. 2008;33:491-500.

16. Arac D, Boucard AA, Bolliger MF, Nguyen J, Soltis SM, Sudhof TC, et al. A novel evolutionarily conserved domain of cell-adhesion GPCRs mediates autoproteolysis. EMBO J. 2012;31:1364-78.

17. Lin HH, Chang GW, Davies JQ, Stacey M, Harris J, Gordon S. Autocatalytic cleavage of the EMR2 receptor occurs at a conserved G protein-coupled receptor proteolytic site motif. J Biol Chem. 2004;279:31823-32.

18. Petersen SC, Luo R, Liebscher I, Giera S, Jeong SJ, Mogha A, et al. The adhesion GPCR GPR126 has distinct, domain-dependent functions in Schwann cell development mediated by interaction with laminin-211. Neuron. 2015;85:755-69.

19. Liebscher I, Schon J, Petersen SC, Fischer L, Auerbach N, Demberg LM, et al. A tethered agonist within the ectodomain activates the adhesion G protein-coupled receptors GPR126 and GPR133. Cell Rep. 2014;9:2018-26.

20. Stoveken HM, Hajduczok AG, Xu L, Tall GG. Adhesion G protein-coupled receptors are activated by exposure of a cryptic tethered agonist. Proc Natl Acad Sci U S A. 2015;112:6194-9.

21. Demberg LM, Rothemund S, Schoneberg T, Liebscher I. Identification of the tethered peptide agonist of the adhesion G protein-coupled receptor GPR64/ADGRG2. Biochem Biophys Res Commun. 2015;464:743-7.

22. Kishore A, Purcell RH, Nassiri-Toosi Z, Hall RA. Stalk-dependent and Stalk-independent Signaling by the Adhesion G Protein-coupled Receptors GPR56 (ADGRG1) and BAI1 (ADGRB1). J Biol Chem. 2016;291:3385-94.

23. Lohse MJ, Nuber S, Hoffmann C. Fluorescence/bioluminescence resonance energy transfer techniques to study G-protein-coupled receptor activation and signaling. Pharmacol Rev. 2012;64:299-336.

24. van Unen J, Woolard J, Rinken A, Hoffmann C, Hill SJ, Goedhart J, et al. A Perspective on Studying G-Protein-Coupled Receptor Signaling with Resonance Energy Transfer Biosensors in Living Organisms. Mol Pharmacol. 2015;88:589-95.

25. Haider RS, Godbole A, Hoffmann C. To sense or not to sense-new insights from GPCR-based and arrestin-based biosensors. Curr Opin Cell Biol. 2019;57:16-24.

26. Hauser AS, Avet C, Normand C, Mancini A, Inoue A, Bouvier M, et al. Common coupling map advances GPCR-G protein selectivity. Elife. 2022;11.

27. Avet C, Mancini A, Breton B, Le Gouill C, Hauser AS, Normand C, et al. Effector membrane translocation biosensors reveal G protein and betaarrestin coupling profiles of 100 therapeutically relevant GPCRs. Elife. 2022;11.

28. Masuho I, Ostrovskaya O, Kramer GM, Jones CD, Xie K, Martemyanov KA. Distinct profiles of functional discrimination among G proteins determine the actions of G protein-coupled receptors. Sci Signal. 2015;8:ra123.

29. Masuho I, Skamangas NK, Martemyanov KA. Live cell optical assay for precise characterization of receptors coupling to Galpha12. Basic Clin Pharmacol Toxicol. 2020;126 Suppl 6:88-95.

30. Donthamsetti P, Quejada JR, Javitch JA, Gurevich VV, Lambert NA. Using Bioluminescence Resonance Energy Transfer (BRET) to Characterize Agonist-Induced Arrestin Recruitment to Modified and Unmodified G Protein-Coupled Receptors. Curr Protoc Pharmacol. 2015;70:2 14 1-2

31. Tveden-Nyborg P, Bergmann TK, Jessen N, Simonsen U, Lykkesfeldt J. BCPT Policy for Experimental and Clinical studies. Basic Clin Pharmacol Toxicol. 2021;128:4-8.

32. Jin Z, Tietjen I, Bu L, Liu-Yesucevitz L, Gaur SK, Walsh CA, et al. Disease-associated mutations affect GPR56 protein trafficking and cell surface expression. Hum Mol Genet. 2007;16:1972-85.

33. Kishore A, Hall RA. Disease-associated extracellular loop mutations in the adhesion G protein-coupled receptor G1 (ADGRG1; GPR56) differentially regulate downstream signaling. J Biol Chem. 2017;292:9711-20.

34. Little KD, Hemler ME, Stipp CS. Dynamic regulation of a GPCR-tetraspanin-G protein complex on intact cells: central role of CD81 in facilitating GPR56-Galpha q/11 association. Mol Biol Cell. 2004;15:2375-87.

35. Ohta S, Sakaguchi S, Kobayashi Y, Mizuno N, Tago K, Itoh H. Agonistic antibodies reveal the function of GPR56 in human glioma U87-MG cells. Biol Pharm Bull. 2015;38:594-600.

36. Paavola KJ, Stephenson JR, Ritter SL, Alter SP, Hall RA. The N terminus of the adhesion G protein-coupled receptor GPR56 controls receptor signaling activity. J Biol Chem. 2011;286:28914-21.

37. Singh AK, Lin H-H. The role of GPR56/ADGRG1 in health and disease. Biomedical Journal. 2021.

38. Iguchi T, Sakata K, Yoshizaki K, Tago K, Mizuno N, Itoh H. Orphan G protein-coupled receptor GPR56 regulates neural progenitor cell migration via a G alpha 12/13 and Rho pathway. J Biol Chem. 2008;283:14469-78.

39. Wu MP, Doyle JR, Barry B, Beauvais A, Rozkalne A, Piao X, et al. G-protein coupled receptor 56 promotes myoblast fusion through serum response factor- and nuclear factor of activated T-cell-mediated signalling but is not essential for muscle development in vivo. Febs j. 2013;280:6097-113.

40. Offermanns S, Mancino V, Revel JP, Simon MI. Vascular system defects and impaired cell chemokinesis as a result of Galpha13 deficiency. Science. 1997;275:533-6.

41. Gu JL, Muller S, Mancino V, Offermanns S, Simon MI. Interaction of G alpha(12) with G alpha(13) and G alpha(q) signaling pathways. Proc Natl Acad Sci U S A. 2002;99:9352-7.

42. Riobo NA, Manning DR. Receptors coupled to heterotrimeric G proteins of the G12 family. Trends Pharmacol Sci. 2005;26:146-54.

43. Lutz S, Freichel-Blomquist A, Yang Y, Rumenapp U, Jakobs KH, Schmidt M, et al. The guanine nucleotide exchange factor p63RhoGEF, a specific link between Gq/11-coupled receptor signaling and RhoA. J Biol Chem. 2005;280:11134-9.

44. Welch HC, Coadwell WJ, Ellson CD, Ferguson GJ, Andrews SR, Erdjument-Bromage H, et al. P-Rex1, a PtdIns(3,4,5)P3- and Gbetagamma-regulated guanine-nucleotide exchange factor for Rac. Cell. 2002;108:809-21.

45. Xu L, Begum S, Hearn JD, Hynes RO. GPR56, an atypical G protein-coupled receptor, binds tissue transglutaminase, TG2, and inhibits melanoma tumor growth and metastasis. Proc Natl Acad Sci U S A. 2006;103:9023-8.

46. Zhu B, Luo R, Jin P, Li T, Oak HC, Giera S, et al. GAIN domain-mediated cleavage is required for activation of G protein-coupled receptor 56 (GPR56) by its natural ligands and a small-molecule agonist. J Biol Chem. 2019.

47. Scholz N, Gehring J, Guan C, Ljaschenko D, Fischer R, Lakshmanan V, et al. The adhesion GPCR latrophilin/CIRL shapes mechanosensation. Cell Rep. 2015;11:866-74.

48. Karpus ON, Veninga H, Hoek RM, Flierman D, van Buul JD, Vandenakker CC, et al. Shear stress-dependent downregulation of the adhesion-G protein-coupled receptor CD97 on circulating leukocytes upon contact with its ligand CD55. J Immunol. 2013;190:3740-8.

49. Yeung J, Adili R, Stringham EN, Luo R, Vizurraga A, Rosselli-Murai LK, et al. GPR56/ADGRG1 is a platelet collagen-responsive GPCR and hemostatic sensor of shear force. Proc Natl Acad Sci U S A. 2020;117:28275-86.